

## Sensitivity-based Damage detection in deep water risers using modal parameters: numerical study

Cheonhong Min<sup>\*</sup>, Hyungwoo Kim, Taekyeong Yeu and Sup Hong

Technology Center for Offshore Plant Industries, Korea Research Institute of Ships & Ocean Engineering,  
1312 Yuseong-daro, Yuseong-gu, Daejeon 305-343, Republic of Korea

(Received April 1, 2014, Revised January 19, 2015, Accepted January 19, 2015)

**Abstract.** A main goal of this study is to propose a damage detection technique to detect and localize damages of a top-tensioned riser. In this paper, the top-tensioned finite element (FE) model is considered as an analytical model of the riser, and a vibration-based damage detection method is proposed. The present method consists of a FE model updating and damage index method. In order to accomplish the goal of this study, first, a sensitivity-based FE model updating method using natural frequencies and zero frequencies is introduced. Second, natural frequencies and zero frequencies of the axial mode on the top-tensioned riser are estimated by eigenvalue analysis. Finally, the locations and severities of the damages are estimated from the damage index method. Three numerical examples are considered to verify the performance of the proposed method.

**Keywords:** damage index; deep water riser; damage detection; FE model updating

---

### 1. Introduction

Risers serve a very important use deep-seabed mining: they are used to lift nodules from the deep-seabed to offshore facilities. Unfortunately, risers are also at high risk of being damaged due to their exposure to harsh environmental conditions such as a currents, pressure, high tension, and vortex induced vibration (Fig. 1). Therefore, the ability to preemptively protect a riser's performance as well as detect damage before riser failure, is imperative. For these reasons, an accurate health monitoring method for marine risers should be developed to detect and localize potential damages. This paper deals with the development of a health monitoring method for vertical rigid risers, i.e., top-tensioned riser.

Myriad damage detection methods have been assessed to detect and locate the damages of various risers such as flexible risers, steel catenary risers, and top-tensioned risers. Iranpour *et al.* (2008) developed a fatigue damage estimation method for oil and gas risers under vortex-induced vibration. Riveros *et al.* (2008) examined a statistical pattern recognition technique to identify and locate structural damages of flexible risers using vibration data. Elman and Alvim (2008) conducted laboratory tests to detect damage to armor wires using non-invasive sensors attached to the flexible riser. Wei and Bai (2009) studied an acoustic-based riser monitoring system to predict

---

<sup>\*</sup>Corresponding author, Ph.D., E-mail: [chmin@kriso.re.kr](mailto:chmin@kriso.re.kr)

the fatigue failure caused by vortex induced vibration. Jacques *et al.* (2010) proposed non-destructive testing methods that consist of optical fiber sensors based on Bragg gratings and acoustic emissions to give early warning of damages of flexible risers. Huang *et al.* (2012) proposed a fatigue estimation method in deep water risers: the method was based on wavelet transform and the second order blind identification method. Magnetic flux leakage sensors were used for local monitoring. An integrated autoregressive moving average model method was proposed for the structural health monitoring of subsea pipeline system by Bao *et al.* (2013). Numerical tests were conducted to verify the proposed method. Min *et al.* (2013) proposed sensitivity-based structural health monitoring method for top-tensioned risers without baseline modal parameters. Zero frequencies used as target parameters to supplement the number of design variables for FE model updating. Numerical examples were considered to verify the performance of the proposed method. Kluk *et al.* (2013) proposed a real-time riser fatigue monitoring system (Fig. 2) to provide field measurements of drilling riser stress and fatigue. Two real field tests at 1180 and 1939 meter water depths were carried out to verify the proposed method. Although many methods are studied for health monitoring of deep water risers, most of them mentioned above have some limitations (i.e., limitation of usable sensors at deep water, limitation of system identification methods for ultra-long marine riser at operation condition, low accuracy of damage detection and /or other uncertainties).

To overcome these limitations, vibration-based damage detection method is considered. Vibration-based damage detection methods have been widely used to detect damages in various engineering fields. Many researchers have focused on the changes of natural frequencies or/and mode shapes between undamaged structures and damaged structures (Stubbs *et al.* 1992, Kim and Stubbs 2003, Lee *et al.* 2012). Some investigations have focused on utilizing zero frequencies to improve the accuracy of damage detection methods (Dilena and Morassi 2004, Nam *et al.* 2005).

The main objective of this paper is to propose a new damage detection method for top-tensioned risers with modal parameters of the damaged model. To achieve the stated goal, a sensitivity-based FE updating method with natural frequencies and zero frequencies is applied to update the stiffness matrix of the FE model, and a damage index method is also adopted to detect and locate the damages of top-tensioned risers. Three numerical examples are considered to verify the proposed method.



Fig. 1 End-fitting failure example (Pipa *et al.* 2010)

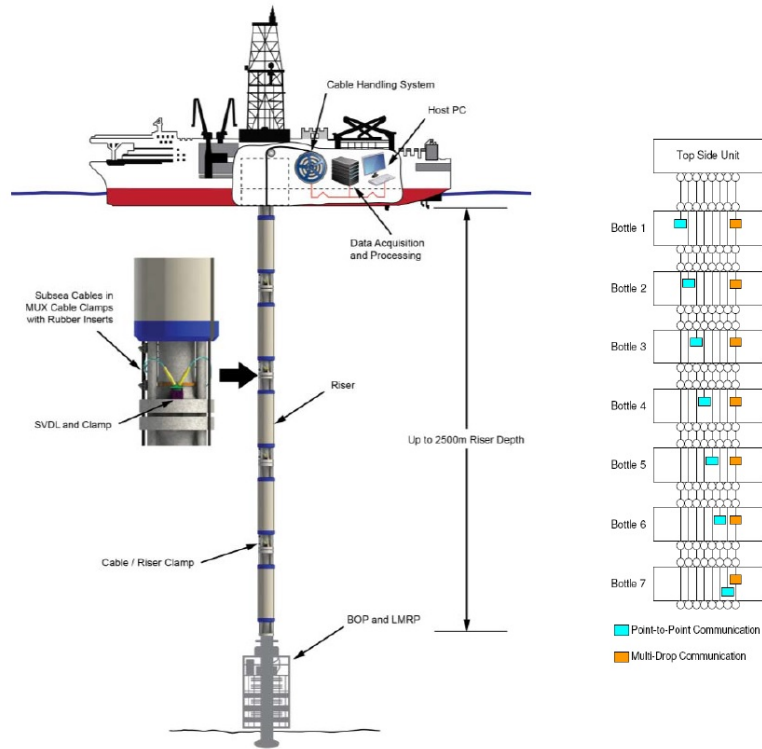


Fig. 2 Real-time riser fatigue monitoring system proposed by Kluk *et al.* (2013)

## 2. Finiteelement model of top-tensioned riser

A two dimensional finite element (FE) structural model is used to obtain the solution for the eigenvalue problem, as well as to evaluate the natural frequencies of the top-tensioned riser. The deep water riser model can be simplified by neglecting the bending stiffness and assuming free rotations at the ends. Thus, application of bar elements to the deep water riser model consist of bar elements is sufficient (Rustad *et al.* 2008). This FE model consists of bar elements; each bar element can be described with four degrees of freedom (DOF): that is two translational DOFs in both ends of the element [see Rustad *et al.* (2008) for details]. All four DOF are shown in Fig. 3:  $x$  is transverse DOF, and  $z$  is axial DOF.

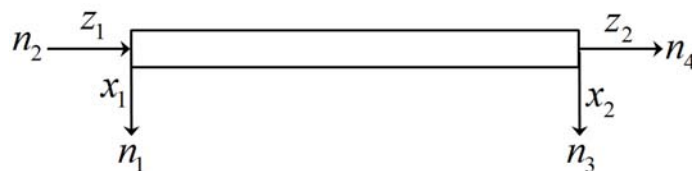


Fig. 3 Bar element with four DOFs

The element stiffness matrix,  $\mathbf{k}$ , consists of two components: the elastic stiffness,  $\mathbf{k}_E$ , and the geometric stiffness,  $\mathbf{k}_G$ . The elastic stiffness matrix is not dependent on the configuration of the structure, while the geometric matrix takes into account changes of the global geometry and the stiffening effect from the axial tension,  $P$ . The elastic stiffness matrix works in the axial direction, whereas the geometric stiffness in the lateral direction. As the water depth increases, the riser will increasingly behave as a cable; the geometric stiffness will become more important than the elastic stiffness (Rustad *et al.* 2008). The element stiffness matrix for the element  $i$ ,  $\mathbf{k}_i$ , has the following form

$$\mathbf{k}_i = \mathbf{k}_{Ei} + \mathbf{k}_{Gi} = \frac{1}{l_i} \left( EA_c \begin{bmatrix} 0 & 0 & 0 & 0 \\ 0 & 1 & 0 & -1 \\ 0 & 0 & 0 & 0 \\ 0 & -1 & 0 & 1 \end{bmatrix} + P_i \begin{bmatrix} 1 & 0 & -1 & 0 \\ 0 & 0 & 0 & 0 \\ -1 & 0 & 1 & 0 \\ 0 & 0 & 0 & 0 \end{bmatrix} \right) \quad (1)$$

where  $E$  is Young's modulus of elasticity,  $A_c$  is the cross-sectional area of the element, and  $l_i$  is the length of element  $i$ . The axial tension  $P_i$  in each element is defined as a function of the elongation of the element  $i$

$$P_i = \frac{EA_c}{l_0} \Delta l_i, \quad \Delta l_i = l_i - l_0 \quad (2)$$

where  $l_0$  is the initial length of an element in an un-tensioned riser.

The element mass matrix,  $\mathbf{m}$ , consists of three terms; the structural mass of the riser,  $\mathbf{m}_s$ , the internal fluid,  $\mathbf{m}_f$ , and the hydrodynamic added mass,  $\mathbf{m}_A$ . The structural mass matrix is given by Eq. (3).

$$\mathbf{m}_{Si} = \frac{\rho_s A_c l_i}{6} \begin{bmatrix} 2 & 0 & 1 & 0 \\ 0 & 2 & 0 & 1 \\ 1 & 0 & 2 & 0 \\ 0 & 1 & 0 & 2 \end{bmatrix} \quad (3)$$

where  $\rho_s$  is the mass density of the riser.

The internal fluid matrix is denoted by Eq. (4).

$$\mathbf{m}_{Fi} = \frac{\rho_f A_{int} l_i}{6} \begin{bmatrix} 2 & 0 & 1 & 0 \\ 0 & 2 & 0 & 1 \\ 1 & 0 & 2 & 0 \\ 0 & 1 & 0 & 2 \end{bmatrix} \quad (4)$$

where  $\rho_f$  is the mass density of the internal fluid,  $A_{int}$  is the internal area of the riser.

The added mass matrix is given by Eq. (5).

$$\mathbf{m}_{Ai} = \frac{\rho_w C_m A_e l_i}{6} \begin{bmatrix} 2 & 0 & 1 & 0 \\ 0 & 0 & 0 & 0 \\ 1 & 0 & 2 & 0 \\ 0 & 0 & 0 & 0 \end{bmatrix} \quad (5)$$

where  $\rho_w$  is the mass density of water,  $C_m$  is hydrodynamic added mass coefficient,  $A_e$  is the external area of the riser. The element stiffness matrix for the element  $i$ ,  $\mathbf{m}_i$ , is written as:

$$\mathbf{m}_i = \mathbf{m}_{Si} + \mathbf{m}_{Fi} + \mathbf{m}_{Ai} \quad (6)$$

### 3. Sensitivity-based damage detection method

#### 3.1 Zero frequencies as additional information

The sensitivity-based methods are widely used methods for FE model updating due to their good performance to reconstruct the measured response quantities, such as natural frequencies, mode shapes, and FRFs. In order to build the correct system matrices, many number of design variables are required, however, available parameters (i.e., natural frequencies and mode shapes) as design variables for FE model updating are very limited.

Many researchers (Mottershead 1998, Rade and Lallement 1998, Jones and Turcotte 2002, Nam *et al.* 2005) reported that zero frequencies are used to supplement the information of vibration characteristics. Zero frequencies are local properties while natural frequencies are global properties, i.e., the same natural frequencies will be occurred on any FRFs of the system. Different FRFs have different zero frequencies, and zero frequencies may be not appeared at some FRFs.

Two DOF mass-spring system is shown in Fig. 4. An individual  $H_{i,j}(\omega)$  is physically defined as the ratio of displacement at coordinate  $i$  to a sole force applied at coordinate  $j$

$$H_{i,j}(\omega) = \sum_{r=1}^N \frac{\phi_{r,i} \phi_{r,j}}{\omega_r^2 - \omega^2} \quad (7)$$

where  $\phi_{r,i}$  and  $\phi_{r,j}$  are the elements  $i$  and  $j$  of the  $r$ th mode shape vector, and  $\omega_r$  is the  $r$ th natural frequency.

$H_{1,1}(\omega)$  of the two DOF system can be expressed by Eq. (8).

$$H_{1,1}(\omega) = \frac{\phi_{1,1}^2}{\omega_1^2 - \omega^2} + \frac{\phi_{2,1}^2}{\omega_2^2 - \omega^2} \quad (8)$$

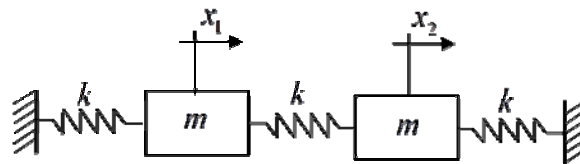


Fig. 4 Mass-spring system with 2 DOFs

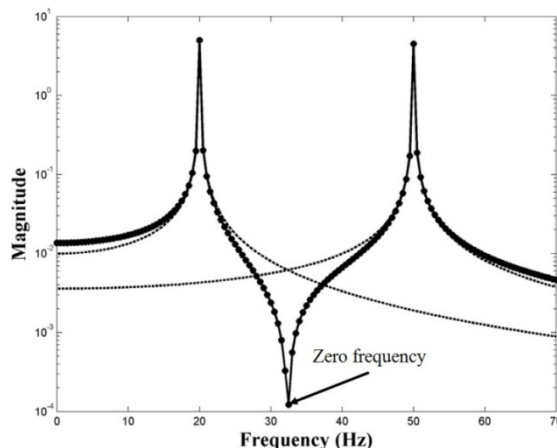


Fig. 5 Zero frequency of an FRF of a 2 DOF Mass-spring system (Min *et al.* 2014)

In case of  $\omega < \omega_1$ , both the first term and the second term of Eq. (8) are positive, and in case of  $\omega > \omega_2$ , both the first term and the second term of Eq. (8) are negative. However, in case of  $\omega_1 < \omega < \omega_2$ , the first term is negative while the second one is positive. Therefore, the two terms are canceled out. So, there will be either a zero frequency or minimum between two resonances frequencies  $\omega_1$  and  $\omega_2$ . When the FRF is plotted on a *dB* or *log* scale, this zero receptance will signify the zero frequency. This is drawn in Fig. 5.

The zero frequencies in  $H_{i,j}$  can be defined the square root of eigenvalues of reduced mass and stiffness matrices. These matrices are formed from original mass and stiffness matrices, but with its  $i$ th row and  $j$ th column removed (Mottershead 1998). The  $H_{i,j}$  matrix consists of diagonal elements,  $H_{1,1}, H_{2,2}, \dots, H_{n,n}$ , called point frequency response functions, and the other elements called transfer frequency response functions. Zero frequencies can be obtained from either the point FRFs or the transfer FRFs. While natural frequencies (i.e., peaks in FRFs) are generated at the same locations in frequency axis for all measurement locations, the zeros occur at different frequencies depending on the locations of measurement. Zero frequencies could be abundant and provide additional information regarding the dynamic behavior of a structure.

### 3.2 Sensitivity-based FE model updating with natural frequencies and zero frequencies

Stubbs and Osegueda (1990) presented the sensitivity-based system identification method; the method was extended to accommodate other spectral information (i.e., zero frequencies and static compliance dominant frequencies) by Nam *et al.* (2005). Min *et al.* (2012) applied Nam *et al.*'s (2005) method to the beam structure, and experimental test was conducted to verify the performance of the method.

In this paper, the sensitivity-based FE model updating method of Min *et al.* (2012) is utilized, the method summarized as follows. Note that, in this paper, only changes in stiffness parameters are considered since the change in mass is negligible in common structural damage (e.g., cracks,

time-dependent degradation in concrete structure, loosen connections in steel structure) and the effect of change in damping parameters on change in spectral information is negligibly small.

A marine riser FE model consists of  $p$  elements, then the sensitivity matrix can be calculated in the following manner. First,  $m$  natural frequencies and  $n$  zero frequencies,  $\omega_i (i=1, 2, \dots, m+n)$ , are numerically generated for the initial FE model. Second, a known amount of Young's modulus,  $E$ , change at  $j$ th element of the FE model,  $\Delta\gamma_j (j=1, 2, \dots, p)$ , is introduced and the corresponding  $m$  natural frequencies and  $n$  zero frequencies,  $\omega_i^* (i=1, 2, \dots, m+n)$ , are numerically computed. Third, the difference in frequencies between the initial and modified FE models,  $z_i (i=1, 2, \dots, m+n)$ , is obtained by  $z_i = \frac{\omega_i^* - \omega_i}{\omega_i}$ . Fourth, each component of the  $j$ th column of the sensitivity matrix,  $\mathbf{S}$ , is computed dividing the change in each frequency by the simulated severity at element  $j$ . Finally, the sensitivity matrix is generated by repeating the above procedure for all  $p$  elements. The complete sensitivity matrix is given by

$$\mathbf{S} = \begin{bmatrix} \frac{z_1}{\Delta\gamma_1} & \frac{z_1}{\Delta\gamma_2} & \dots & \frac{z_1}{\Delta\gamma_p} \\ \frac{z_2}{\Delta\gamma_1} & \frac{z_2}{\Delta\gamma_2} & \dots & \frac{z_2}{\Delta\gamma_p} \\ \vdots & \vdots & \ddots & \vdots \\ \frac{z_{m+n}}{\Delta\gamma_1} & \frac{z_{m+n}}{\Delta\gamma_2} & \dots & \frac{z_{m+n}}{\Delta\gamma_p} \end{bmatrix} \quad (9)$$

Once the sensitivity matrix is constructed using the initial FE model, and the natural frequencies and the zero frequencies extracted from experiment, i.e., target parameters to be matched, are available, the optimal solution of FE model updating problem can be deduced by solving the linear equations expressed by

$$\alpha = \mathbf{S}^{-1}\mathbf{Z} \quad (10)$$

where  $\mathbf{Z}$  is a  $(m+n) \times 1$  column matrix representing the difference in frequencies between the initial FE model and the modified FE model, and  $\alpha$  is a  $p \times 1$  column matrix that there are  $p$  unknown Young's modulus parameters to be updated into the FE model. The sensitivity matrix,  $\mathbf{S}$ , is usually not a square matrix that is required to find the minimum square solution like pseudo-inverse. For a structurally-underdetermined system that involves more unknowns than the number of equations (i.e.,  $m+n < p$ ), the inverse solution is the minimal norm and may not be unique.

The Young's modulus of each element  $j$  of the FE model is then updated by the following equation

$$E_j^* = E_j (1 + \alpha_j) \quad (11)$$

where  $E_j$  is the known Young's modulus of the  $j$ th element of the initial FE model,  $\alpha_j$  is the

fractional change of Young's modulus solved by Eq. (10), and  $E_j^*$  is a new Young's modulus of the updated FE model. With the updated FE model, an eigenvalue analysis is performed to generate new natural frequencies for the next step. This process is repeated until  $\mathbf{Z}$  is satisfied with an allowable error or  $\alpha \approx 0$ , i.e., the system converges.

The proposed sensitivity-based FE model updating method can be summarized as follows:

1. Obtain the natural and zero frequencies from the target structure (i.e., an existing structure) via experimental modal analysis;
2. Build an initial FE model that corresponds to the real structure by utilizing all the possible knowledge about design and construction of the structure;
3. Compute the natural and zero frequencies of the initial FE model;
4. Identify the difference in frequencies between the initial FE model and the target structure, i.e., compute  $\mathbf{Z}$ ;
5. Compute the sensitivity matrix,  $\mathbf{S}$ , using the initial FE model;
6. Estimate the Young's modulus changes by first solving Eq. (10) and fine-tune the FE model by solving Eq. (11); and
7. Repeat steps (3)-(6) until  $\mathbf{Z}$  is satisfied with an allowable error or system converges when the elastic modulus of the updated FE model are identical to those of the real structure.

### 3.3 Damage index method

The damage index method utilizes the change in modal parameters such as natural frequencies and mode shapes of the pre-damaged and post-damaged structures to detect and locate damages (Stubbs *et al.* 1992, Kim and Stubbs 2002, Li *et al.* 2014, You *et al.* 2014). In this paper, the damage index method is modified to detect damages of the top-tensioned riser without modal parameters of undamaged structures. The damage index for the  $i$ th element,  $DI_i$ , can be expressed as

$$DI_i = \frac{E_{i,int}}{E_{i,up}} \quad (12)$$

where  $E_{i,int}$  is the Young's modulus of the  $i$ th element of the initial FE model and  $E_{i,up}$  is the Young's modulus of the  $i$ th element of the updated FE model.

To further generalize the  $DI_i$  independently of the structure type, the normalized  $DI_i$ ,  $NDI_i$ , is given by

$$NDI_i = \frac{DI_i - \mu_{DI}}{\sigma_{DI}} \quad (13)$$

where  $\mu_{DI}$  and  $\sigma_{DI}$  represent mean and standard deviation of the damage index, respectively. To classify whether damage exists in a specific element,  $NDI_i$  should be compared with a threshold value,  $\eta$ .

### 3.4 Procedure for Damage detection

Fig. 6 shows the flowchart of the damage detection of the top-tensioned riser. Nine steps are utilized to detect the damages, and these steps are described below.

1. Select a real structure;
2. Perform a modal testing to obtain the accelerance FRFs of the structure;
3. Extract modal parameters (i.e., natural frequencies,  $EXP(\omega_n)$  and zero frequencies,  $EXP(\omega_z)$ ) of the structure using modal parameter identification methods;
4. Make a FE model corresponding real structure using initial properties;
5. Perform eigenvalue analysis to obtain the natural frequencies of FE model,  $FEM(\omega_n)$ , and the zero frequencies of FE model,  $FEM(\omega_z)$ ;
6. Select the updating parameters, Young's modulus of FE model, and target parameters,  $EXP(\omega_n)$  and  $EXP(\omega_z)$ ;
7. Perform sensitivity-based FE model updating to get modified stiffness matrices;
8. Obtain the updated stiffness matrices; and
9. Finally, detect damages using Eqs. (12) and (13)

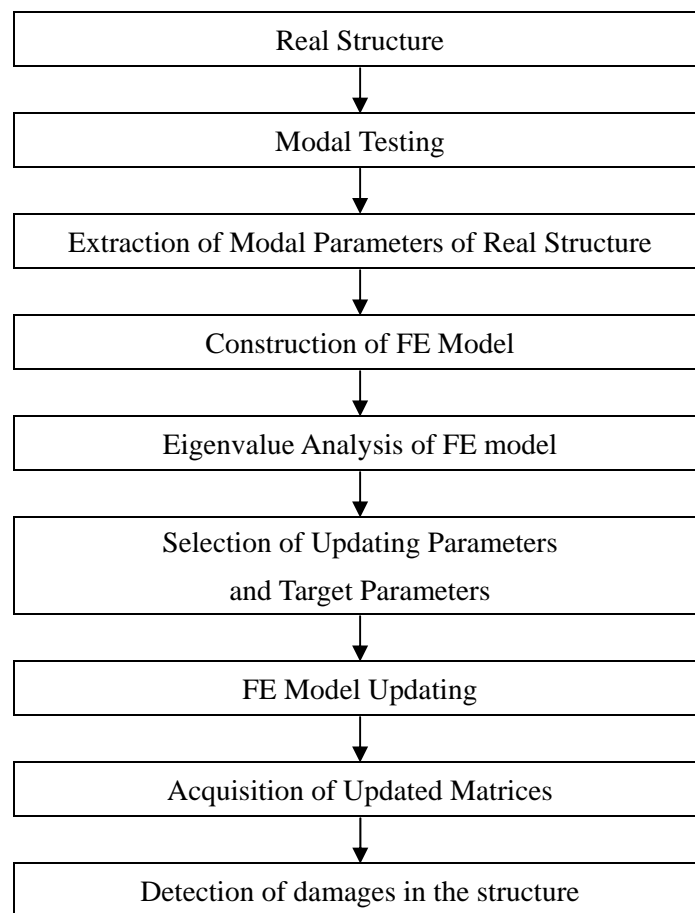


Fig. 6 Flowchart of the of the damage detection of the top-tensioned rise

## 4. Numerical examples

### 4.1 Description of the numerical model

An analytical model of a typical top-tensioned vertical riser depicted in Fig. 7 is considered to verify the effectiveness of the proposed method. The model assumes conditions for both directions at its bottom end; the top node is free in the vertical direction, only affected by the top tension acting as a vertical force. The material properties and geometric information of the riser are listed in Table 1.

The FE model consists of 20 elements and 21 nodes; structural damping is not considered. The FE model is considered as a base model for numerical examples. Eigenvalue analysis is carried out to obtain the natural frequencies of the base model.

Table 1 Properties and geometric information of the riser

Property	Base beam
Riser length	2200 m
Outside/Inside diameter	0.23/ 0.2 m
Top tension	1800 kN
Riser material density	7860 kg/m <sup>3</sup>
Sea water density	1025 kg/m <sup>3</sup>
Riser internal fluid density	800 kg/m <sup>3</sup>
Riser material Young's modulus	203 GPa
Added mass coefficient	1

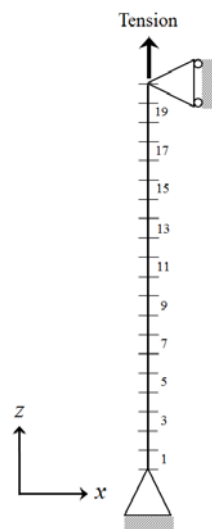


Fig. 7 Fixed-roller vertical riser model with top-tension

#### 4.2 Damage detection

In order to examine the accuracy and efficiency of the proposed damage detection method, three scenarios listed in Table 2 are investigated to represent different damage characteristics (location and damage severity). For all scenarios, damage is inflicted in the structure via reducing the Young's modulus of the appropriate elements. Assumption of the Young's modulus reduction can represent the damages at the deep water riser such as corrosion, erosion and cracks. In the first scenario, the damage is limited to one location in the structure, and 30% of Young's modulus in element 1 (Case 1) is reduced to simulate damage. In damage case2, two damage locations are considered. In damage case 3, four elements are damaged; the damage severity ranges from 10% to 25%.

Table 2 Damage scenarios

Damage scenario	Damage location	Damage severity (%)
Case 1	E1	30
Case 2	E5, E15	30, 30
Case 3	E5, E10, E11, E15	10, 15, 20, 25

Table 3 Natural frequencies of the lateral and axial mode

No.	Natural frequency (Hz)							
	Undamaged		Case 1		Case 2		Case 3	
	Lateral mode	Axial mode	Lateral mode	Axial mode	Lateral mode	Axial mode	Lateral mode	Axial mode
1	0.019	0.503	0.019	0.493	0.019	0.492	0.019	0.494
2	0.038	1.513	0.038	1.482	0.038	1.476	0.038	1.473
3	0.057	2.532	0.057	2.483	0.057	2.495	0.057	2.477
4	0.077	3.567	0.077	3.503	0.077	3.517	0.077	3.514
5	0.097	4.624	0.097	4.548	0.097	4.493	0.097	4.526
6	0.118	5.709	0.118	5.625	0.118	5.533	0.118	5.545
7	0.140	6.828	0.140	6.740	0.140	6.777	0.140	6.724
8	0.162	7.988	0.162	7.899	0.162	7.931	0.162	7.884
9	0.185	9.194	0.185	9.106	0.185	8.909	0.185	8.973
10	0.210	10.450	0.210	10.365	0.210	10.127	0.210	10.145

Eigenvalue analyses is carried out to obtain natural frequencies of the post-damaged structures. The first 10 natural frequencies of the axial mode and lateral mode are listed in Table 3. Changes of the lateral mode natural frequencies are very little in damage cases (i.e., the lateral mode natural frequencies have very low sensitivity to changes of Young's modulus), but the natural frequencies of the axial mode are shifted depending on the damage scenarios. In the case of the top-tensioned riser, it is effective to use the modal parameters extracted from the axial modes for damage detection because the Young's modulus of the riser affecting the axial direction.

In this paper, the performance of the approach using additional information is compared with the approach using only natural frequencies via the FE model of the top-tensioned riser. First, the FE model updating is performed using 10 natural frequencies of the axial mode shown in Table 3.

The next, model updating is carried out using the proposed method with natural frequencies and zero frequencies. The 10 natural frequencies and 30 zero frequencies of the axial mode shown in Table 4 are considered as target parameters. Regarding the zero frequencies, 10 zero frequencies are generated from each FRF,  $H_{5,5}$ ,  $H_{10,10}$  and  $H_{15,15}$ , respectively.  $H_{i,j}$  means  $i$ th row and  $j$ th column components of FRF matrix.

The model updating results using 10 natural frequencies are summarized in Table 5; the results obtained with 10 natural frequencies and 30 zero frequencies are listed in Tables 6-8, respectively. The accuracy of the FE model updating results might be compared via maximum percent errors in the finally updated parameters (i.e., natural frequencies and zero frequencies) with respect to the target values. The percent error is defined as

$$\text{Error}(\%) = \frac{|\text{Updated} - \text{Target}|}{\text{Target}} \times 100 \quad (14)$$

Table 4 Natural frequencies and zero frequencies of the axial mode of the base model

Natural frequency (Hz)	Zero Frequency (Hz)		
	$H_{5,5}$	$H_{10,10}$	$H_{15,15}$
0.503	1.513	0.671	1.513
1.513	2.532	2.021	2.532
2.532	3.567	3.393	3.567
3.567	4.624	4.093	4.624
4.624	5.709	4.802	5.709
5.709	6.828	6.263	6.828
6.828	7.988	7.791	7.988
7.988	9.194	8.587	9.194
9.194	10.450	9.399	10.450
10.450	11.758	11.097	11.758

Table 5 Results of FE model updating using natural frequencies

No.	Case 1		Case 2		Case 3	
	Target NF (Hz)	Updated NF (Hz)	Target NF (Hz)	Updated NF (Hz)	Target NF (Hz)	Updated NF (Hz)
1	0.493	0.493	0.492	0.492	0.494	0.494
2	1.482	1.482	1.476	1.476	1.473	1.473
3	2.483	2.483	2.495	2.495	2.477	2.477
4	3.503	3.503	3.517	3.517	3.514	3.512
5	4.548	4.548	4.493	4.493	4.526	4.526
6	5.625	5.625	5.533	5.534	5.545	5.548
7	6.740	6.740	6.777	6.776	6.724	6.721
8	7.899	7.899	7.931	7.930	7.884	7.881
9	9.106	9.106	8.909	8.911	8.973	8.974
10	10.365	10.365	10.127	10.129	10.145	10.150
Max. error (%)	0.003		0.029		0.049	

NF – natural frequencies

From Table 5, the maximum updating errors of natural frequencies in Cases 1-3 are 0.003%, 0.029% and 0.049%, respectively. From Table 6 to Table 8, the maximum updating errors of natural frequencies and zero frequencies in three damage scenarios are 0.004%, 0.004% and 0.001%, respectively.

Table 6 Results of FE model updating using natural frequencies and zero frequencies for Case 1

No.	Target NF (Hz)	Updated NF (Hz)	Target ZF (Hz), $H_{5,5}$	Updated ZF (Hz), $H_{5,5}$	Target ZF (Hz), $H_{10,10}$	Updated ZF (Hz), $H_{10,10}$	Target ZF (Hz), $H_{15,15}$	Updated ZF (Hz), $H_{15,15}$
1	0.494	0.494	1.482	1.482	0.671	0.671	1.482	1.482
2	1.506	1.506	2.483	2.483	2.021	2.021	2.483	2.483
3	2.530	2.530	3.503	3.503	3.393	3.393	3.503	3.503
4	3.519	3.519	4.548	4.548	3.821	3.821	4.548	4.548
5	4.531	4.531	5.625	5.625	4.802	4.802	5.625	5.625
6	5.652	5.652	6.740	6.740	6.263	6.263	6.740	6.740
7	6.826	6.826	7.899	7.898	7.791	7.791	7.899	7.898
8	7.935	7.935	9.106	9.105	8.228	8.227	9.106	9.105
9	9.026	9.026	10.365	10.365	9.399	9.399	10.365	10.365
10	10.307	10.307	11.678	11.677	11.097	11.096	11.678	11.677
Max. error (%)	0.004							

ZF – zero frequencies

Table 7 Results of FE model updating using natural frequencies and zero frequencies for Case 2

No.	Target NF (Hz)	Updated NF (Hz)	Target ZF (Hz), $H_{5,5}$	Updated ZF (Hz), $H_{5,5}$	Target ZF (Hz), $H_{10,10}$	Updated ZF (Hz), $H_{10,10}$	Target ZF (Hz), $H_{15,15}$	Updated ZF (Hz), $H_{15,15}$
1	0.492	0.492	1.476	1.476	0.666	0.666	1.476	1.476
2	1.476	1.476	2.495	2.495	1.967	1.967	2.495	2.495
3	2.495	2.495	3.517	3.517	3.387	3.387	3.517	3.517
4	3.517	3.517	4.493	4.493	3.821	3.821	4.493	4.493
5	4.493	4.493	5.533	5.533	4.721	4.721	5.533	5.533
6	5.533	5.533	6.777	6.777	6.138	6.138	6.777	6.777
7	6.777	6.777	7.931	7.932	7.791	7.791	7.931	7.932
8	7.931	7.932	8.909	8.909	8.227	8.228	8.909	8.909
9	8.909	8.909	10.127	10.127	9.188	9.188	10.127	10.127
10	10.127	10.127	11.694	11.694	10.970	10.970	11.694	11.694
Max. error (%)	0.004							

Table 8 Results of FE model updating using natural frequencies and zero frequencies for Case 3

No.	Target NF (Hz)	Updated NF (Hz)	Target ZF (Hz), $H_{5,5}$	Updated ZF (Hz), $H_{5,5}$	Target ZF (Hz), $H_{10,10}$	Updated ZF (Hz), $H_{10,10}$	Target ZF (Hz), $H_{15,15}$	Updated ZF (Hz), $H_{15,15}$
1	0.494	0.494	1.473	1.473	0.653	0.653	1.473	1.473
2	1.473	1.473	2.477	2.477	1.977	1.977	2.477	2.477
3	2.477	2.477	3.514	3.514	3.316	3.316	3.514	3.514
4	3.514	3.514	4.526	4.526	4.014	4.014	4.526	4.526
5	4.526	4.526	5.545	5.545	4.665	4.665	5.545	5.545
6	5.545	5.545	6.724	6.724	6.125	6.125	6.724	6.724
7	6.724	6.724	7.884	7.884	7.657	7.657	7.884	7.884
8	7.884	7.884	8.973	8.973	8.472	8.472	8.973	8.973
9	8.973	8.973	10.145	10.145	9.127	9.127	10.145	10.145
10	10.145	10.145	11.618	11.618	10.816	10.816	11.618	11.618
Max. error (%)	0.001							

In each updating process, Young's modulus of all elements are iteratively updated until  $\alpha < 10^{-3}$ . The updating results of three cases are given in Table 9. From Table 9, the maximum errors in the finally updated FE model obtained when using only 10 natural frequencies are 28.4%, 16.09%, and 16.92% for Case 1, Case 2 and Case 3, respectively; the maximum errors using zero frequencies are 0.02%, 0.02%, and 0.06% for Cases 1-3, respectively. The results show that the proposed FE model updating technique is quite effective for model updating and it is a feasible approach for identifying Young's modulus of structures.

Table 9 Results of FE model updating

Element number	Case 1			Case 2			Case 3		
	Target E (GPa)	Updated E using NF	Updated E using NF and ZF	Target E (GPa)	Updated E using NF	Updated E using NF and ZF	Target E (GPa)	Updated E using NF	Updated E using NF and ZF
1	142.1	182.46	142.07	203.00	196.00	203.01	203.00	192.80	203.05
2	203.00	181.85	202.99	203.00	191.93	202.98	203.00	193.12	203.01
3	203.00	204.97	202.98	203.00	196.39	202.99	203.00	195.62	202.99
4	203.00	192.08	203.01	203.00	194.17	203.00	203.00	195.54	202.96
5	203.00	201.77	202.99	142.1	162.09	142.10	182.7	187.22	182.68
6	203.00	193.84	202.97	203.00	235.57	203.01	203.00	225.35	203.01
7	203.00	200.72	202.98	203.00	197.07	203.00	203.00	193.74	202.98
8	203.00	194.51	202.98	203.00	194.83	203.01	203.00	195.84	203.00
9	203.00	200.32	203.00	203.00	198.23	203.00	203.00	194.15	202.95
10	203.00	194.74	202.99	203.00	197.03	203.00	172.55	200.39	172.55
11	203.00	200.24	202.99	203.00	193.98	203.01	162.40	189.87	162.42
12	203.00	194.67	202.99	203.00	192.82	203.01	203.00	195.96	202.96
13	203.00	200.46	202.97	203.00	196.12	203.01	203.00	194.26	203.00
14	203.00	194.26	202.98	203.00	194.06	203.01	203.00	196.44	202.97
15	203.00	201.10	202.98	142.10	162.16	142.13	152.25	168.80	152.28
16	203.00	193.21	203.27	203.00	235.66	203.00	203.00	203.13	202.96
17	203.00	202.86	202.97	203.00	196.95	203.00	203.00	194.63	202.94
18	203.00	190.15	203.03	203.00	194.55	203.01	203.00	194.46	203.00
19	203.00	213.91	203.02	203.00	199.16	202.99	203.00	197.02	202.97
20	203.00	212.39	202.71	203.00	194.99	203.03	203.00	197.33	203.12
Max. error (%)		28.4	0.02		16.09	0.02		16.92	0.06

The damage index method is used to locate potential damage in the structure. The normalized damage indices obtained from Eq. (13) are shown in Figs. 3-7. The negative indices are related to undamaged cases; positive indices identify a potentially damaged element: the main task is selecting an adequate threshold level to detect the real damaged elements. If this acceptance criterion is placed too high ( $\eta = 1.5$ ), some damage will not be revealed. At a more proper level ( $\eta = 1$ ), clear discrimination will result. If the acceptance criterion is too low ( $\eta = 0.5$ ), several false detections will result (Alvandi and Cremona 2006). Note that the values of damage threshold, 3, 2 and 1 correspond to the confidence levels of 99.87%, 98% and 84% for the presence of damage, respectively (Park *et al.* 2011). For all damaged cases, the threshold value is selected at 1. From Figs. 8 and 9, both FE model updating using only natural frequencies and FE model updating with natural frequencies and zero frequencies detect damaged elements of Case 1 and Case 2. Fig. 10(a) shows that only one damaged element (i.e., at element 15) is localized by FE model updating using only natural frequencies, but prediction of three damaged elements (i.e., at element 5, 10 and 11) is failed. On the contrary, Fig. 5(b) shows that damaged elements of all cases are perfectly detected except the element 5 of Case 3, however,  $NDI_5$  of Case 3 is just little smaller than threshold value, 1. No false-positive predictions are occurred in any cases.

The damage severities are obtained by Eq. (13).

$$\text{DamageSeverity}(\%) = \frac{\text{Updated}(E)}{\text{Initial}(E)} \times 100 \quad (15)$$

The results of the damage severities for three damage scenarios are presented in Figs.11-13. From Figs.11-13, damage severity estimation results obtained when using 10 natural frequencies as target parameters are predicted at lower levels than true damage severity, while the results by 10 natural frequencies and 30 zero frequencies are estimated accurately for all damage cases.

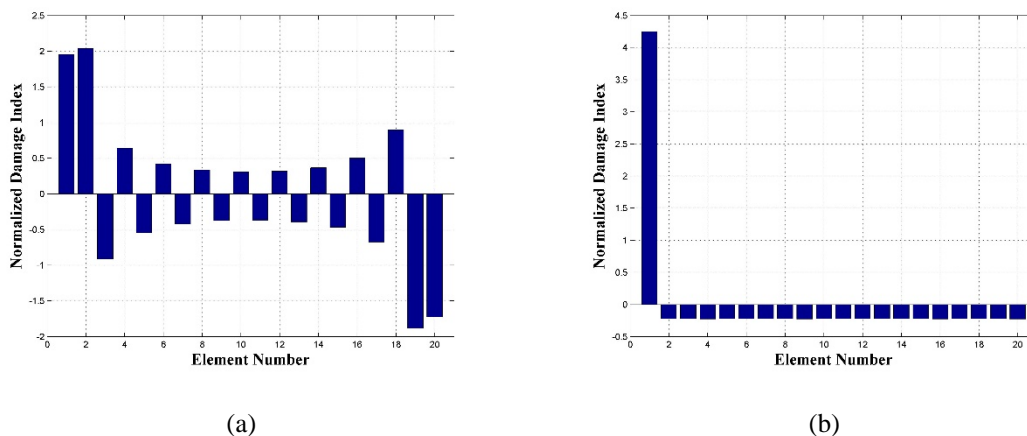


Fig. 8 Damage localization results for damage scenario Case 1. (a) using natural frequencies, (b) using natural frequencies and zero frequencies

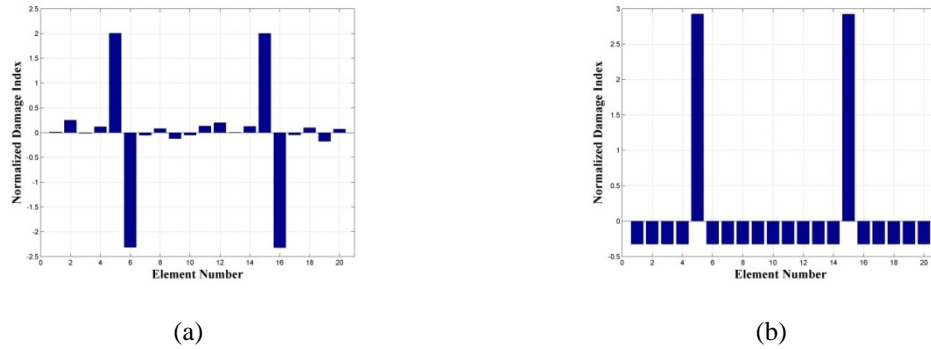


Fig. 9 Damage localization results for damage scenario Case 2. (a) using natural frequencies, (b) using natural frequencies and zero frequencies

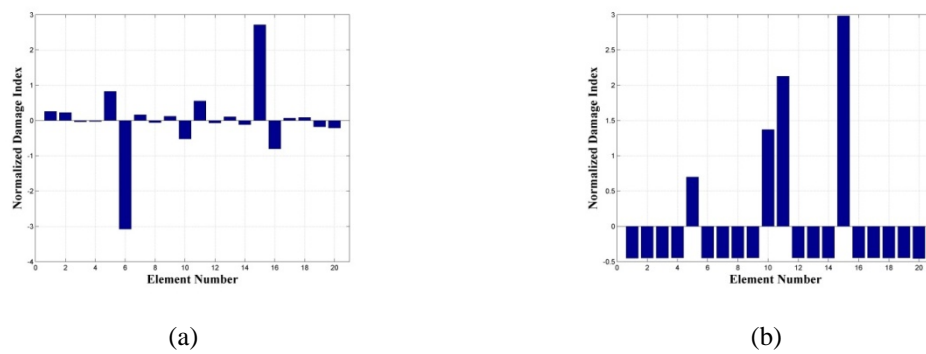


Fig. 10 Damage localization results for damage scenario Case 3. (a) using natural frequencies, (b) using natural frequencies and zero frequencies

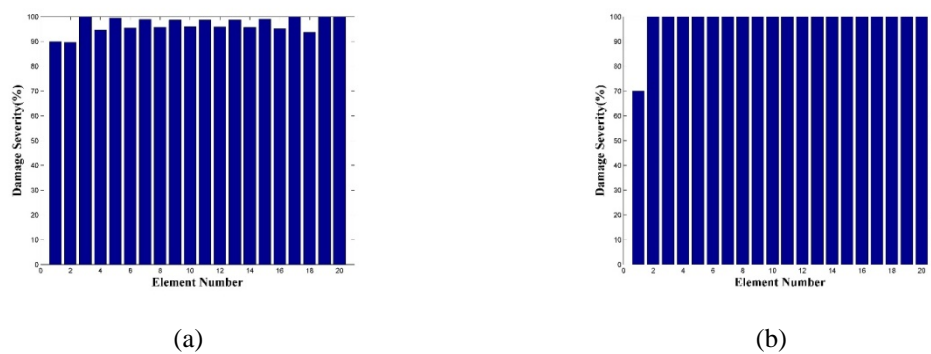


Fig. 11 Damage severity results for damage scenario Case 1. (a) using natural frequencies, (b) using natural frequencies and zero frequencies

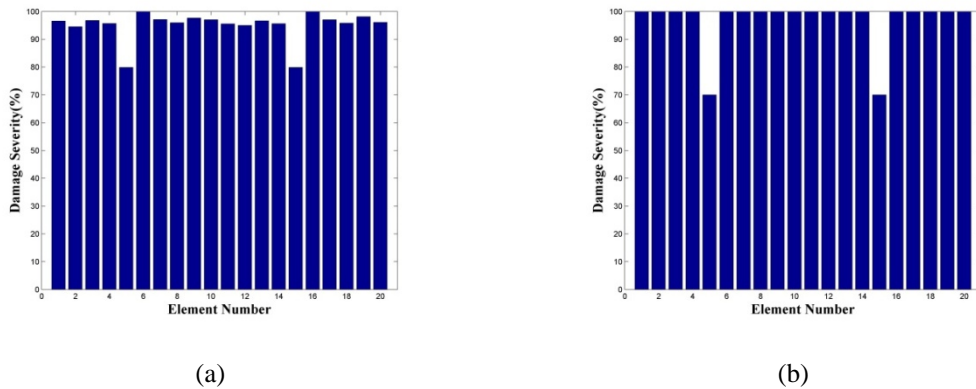


Fig. 12 Damage severity results for damage scenario Case 2. (a) using natural frequencies, (b) using natural frequencies and zero frequencies

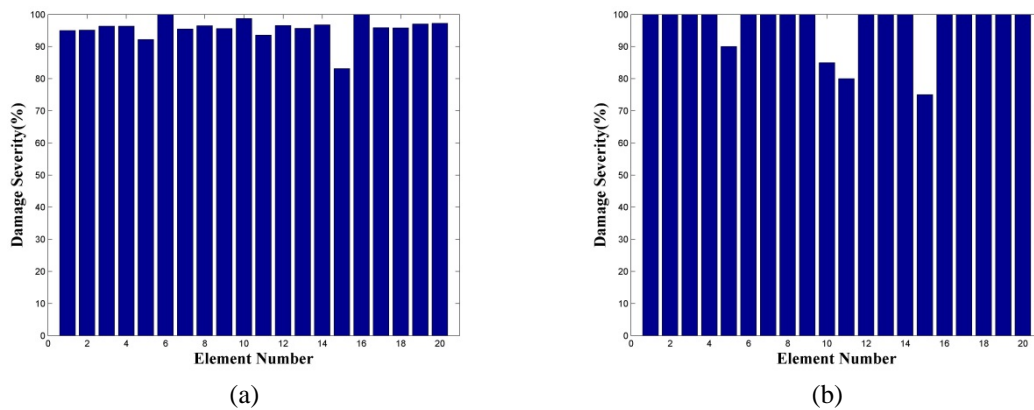


Fig. 13 Damage severity results for damage scenario Case 3. (a) using natural frequencies, (b) using natural frequencies and zero frequencies

## 5. Conclusions

This paper presented a damage detection approach for the top-tensioned riser without pre-damaged response data. The proposed method consists of a FE model updating method and damage index method. A finite element model representing the top-tensioned riser was also developed to simulate three damage cases. Young's modulus of each element was changed through the sensitivity-based FE model updating with natural frequencies and zero frequencies. The damage locations and severities were identified by the damage index method.

The accuracy of the proposed method was numerically verified by several damage scenarios, including both single-damage and multiple-damage scenarios, associated with marine risers. Based

on the numerical studies, the following conclusions are drawn: (1) the natural frequencies and zero frequencies of the axial mode are effective parameters for damage detection of the riser; (2) the numerical simulations of the top-tensioned riser reveal that the use of zero frequencies can reduce errors greatly by removing the ill-conditioning of updating equations; (3) the proposed method can detect and localize single damage and multiple damages of the riser with knowledge of only post-damage modal parameters ; (4) the damage severity of the riser can be estimated by the proposed method.

To apply the proposed method to real deep water risers, more research studies are needed. The key issue of application for these findings to the deep water riser will be measuring the zero frequencies in the field. Although many monitoring tests have been conducted on deep water risers both in the field and laboratory, a method to measure the zero frequencies is still pending. More extensive study on monitoring systems, including usable sensors in deep water, is needed to apply the proposed method to riser in real situation.

## Acknowledgments

This study was initiated by the R&D Project, Technology Development of Deep-Seabed Mining System for Manganese Nodules sponsored by Ministry of Oceans and Fisheries of Korea.

## References

- Alvandi, A. and Cremona, C. (2006), "Assessment of vibration-based damage identification techniques", *J Sound Vib.*, **292**(1-2), 179-202.
- Bao, C., Hao, H. and Li, Z.X. (2013), "Integrated ARMA model method for damage detection of subsea pipeline system", *Eng. Struct.*, **48**, 176-192.
- Dilena, M. and Morassi, A. (2004), "The use of anti resonances for crack detection in beams", *J Sound Vib.*, **276**, 195-214.
- Elman, P. and Alvim, R. (2008), "Development of a failure detection system for flexible risers", *Proceedings of the 18th International Offshore and Polar Engineering Conference*, Vancouver, Canada, July.
- Huang, C., Nagarajaiah, S. and Varadarajan, N. (2012), "Fatigue estimation in deepwater risers based on wavelets and second order blind identification", *Proceedings of the ASME 31st International Conference on Ocean, Offshore and Arctic Engineering*, Rio de Janeiro, Brazil, July.
- Iranpour, M., Taheri, F. and Vandiver, J.K. (2008), "Structural life assessment of oil and gas risers under vortex-induced vibration", *Marine Struct.*, **21**(4), 353-373.
- Jacques, R., Clarke, T., Morikawa, S. and Strohaecker, T. (2010), "Monitoring the structural integrity of a flexible riser during dynamic loading with a combination of non-destructive testing methods", *NDT&E Int.*, **43**(6), 501-506.
- Jones, K. and Turcotte, J., (2002), "Finite element model updating using antiresonant frequencies", *J. Sound Vib.*, **252**(4), 717-727.
- Kim, J.T. and Stubbs, N. (2002), "Improved damage identification method based on modal information", *J Sound Vib.*, **252**(2), 223-238.
- Kim, J.T. and Stubbs, N. (2003), "Crack detection in beam-type structures using frequency data", *J Sound Vib.*, **259**(1), 145-160.
- Kluk, D.J., McNeill, S.I., Bhalla, K.K., Saruhashi, T., Sawada, I., Kyo, M., Miyazaki, E. and Yamazaki, Y. (2013), "Development of a real-time riser fatigue monitoring system", *Proceedings of the Offshore Technology Conference*, Houston, Texas, USA, May.

- Lee, S.Y., Nguyen, K.D., Huynh, T.C., Kim, J.T., Yi, J.H. and Han, S.H. (2012), "Vibration-based damage monitoring of harbor caisson structure with damaged foundation-structure interface", *Smart Struct. Syst.*, **10**(6), 517-546.
- Li, H.M., Yi, T.H., Ren, L.R., Li, D.S. and Huo, L.S. (2014), "Reviews on innovations and applications in structural health monitoring for infrastructures", *Smart Monit. Maint.*, **1**(1), 1-45.
- Min, C.H., Park, S.Y. and Park, H.I. (2012), "Finite element model updating with experimental natural frequency and zero frequency", *Int. J. Offshore Polar*, **22**(3), 225-233.
- Min, C.H., Sup, H., Kim, H.W., Choi, J.S. and Yeu, T.K. (2013), "Structural health monitoring for top-tensioned riser with response data of damaged model", *Proceedings of the 10th ISOPE Ocean Mining and Gas Hydrates Symposium*, Szczecin, Poland, September.
- Min, C.H., Sup, H., Park, S.Y. and Park, D.C. (2014), "Sensitivity-based finite element model updating with natural frequencies and zero frequencies for damped beam structures", *Int. J. Nav. Archit. Ocean Eng.*, **6**(4), 904-921.
- Mottershead, J.E. (1998), "On the zeros of structural frequency response functions and their sensitivities", *Mech. Syst. Signal Pr.*, **12**(5), 591-597.
- Nam, D.H., Choi, S.H., Park, S.Y. and Stubbs, N. (2005), "Improved parameter identification using additional spectral information", *Int. J. Solids Struct.*, **42**(18-19), 4971-4987.
- Park, S.Y., Park, D.C., Kim, E.H. and Kim, H.S. (2011), "Damage evaluation on a jacket platform structure using modal properties", *Proceedings of the 21st International Offshore and Polar Engineering Conference*, Maui, Hawaii, USA, June.
- Pipa, D., Morikawa, S., Pires, G., Camerini, C. and Santos, J.M. (2010), "Flexible riser monitoring using hybrid magnetic/optical strain gage techniques through RLS adaptive filtering", *EURASIP J Advances in Signal Processing*, **2010**, Article ID 176203.
- Rade, D.A. and Lallement, G. (1998), "A strategy for the enrichment of experimental data as applied to an inverse eigensensitivity-based FE model updating method", *Mech. Syst. Signal Pr.*, **12**(2), 293-307.
- Riveros, C., Utsunomiya, T., Maeda, K. and Itoh, K. (2008), "Damage detection in flexible risers using statistical pattern recognition techniques", *Int. J. Offshore Polar*, **18**(1), 35-42.
- Rustad, A.M., Larsen, C.M. and Sorensen, A.J. (2008), "FEM modeling and automatic control for collision prevention of top tensioned risers", *Marine Struct.*, **21**, 80-112.
- Stubbs, N. and Osegueda, R. (1990), "Global non-destructive damage evaluation in solids", *Int. J. Anal. Exper. Modal Anal.*, **5**, 67-79.
- Stubbs, N., Kim, J.T. and Topole, K.G. (1992), "An efficient and robust algorithm for damage localization in offshore platforms", *Proceedings of the ASCE 10th Structures Congress*, San Antonio, Texas, USA, April.
- Wei, D. and Bai, Y. (2009), "Development of an acoustic-based riser monitoring system", *Proceedings of the ASME 28th International Conference on Ocean, Offshore and Arctic Engineering*, Honolulu, Hawaii, USA, May.
- You, T., Gardoni P. and Hurlbaas, S. (2014), "Iterative damage index method for structural health monitoring", *Smart Monit. Maint.*, **1**(1), 89-110.